Cell Reports

Article

Endogenous PP2A inhibitor CIP2A degradation by chaperone-mediated autophagy contributes to the antitumor effect of mitochondrial complex I inhibition

Graphical abstract

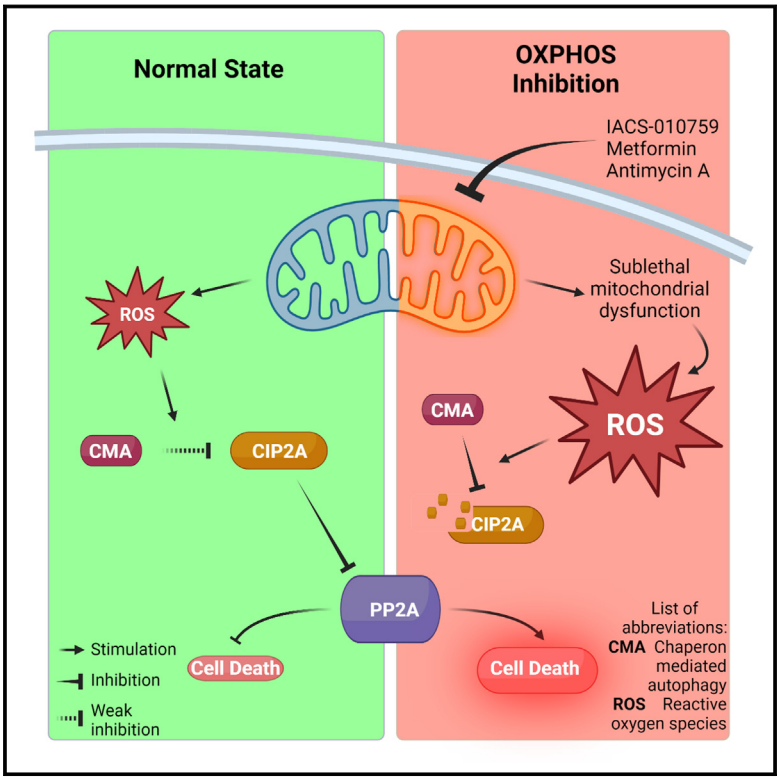

Highlights

- Complex I is a key regulator of CIP2A, a PP2A inhibitor with protumor activity
- Increased mROS mediates the dissociation of CIP2A from PP2A and its degradation
- Hypoglycemia and low dosages of mROS inducers can be exploited as cancer therapy

Authors

Riccardo Cazzoli, Francesco Romeo, Isabella Pallavicini, ..., Marco Foiani, Jukka Westermarck, Saverio Minucci

Correspondence

saverio.minucci@ieo.it

In brief

Cazzoli et al. show that reactive oxygen species production, under low-glucose conditions in combination with low doses of mitochondrial drug inhibitor, enhances CIP2A degradation. CIP2A is an endogenous PP2A inhibitor with a strong prognostic and therapeutic value; more invasive and lethal tumors show increased levels of CIP2A protein.

Cazzoli et al., 2023, Cell Reports *42*, 112616
June 27, 2023
https://doi.org/10.1016/j.celrep.2023.112616

CellPress

Cell Reports

CellPress
OPEN ACCESS

Article

Endogenous PP2A inhibitor CIP2A degradation by chaperone-mediated autophagy contributes to the antitumor effect of mitochondrial complex I inhibition

Riccardo Cazzoli,[1,12] Francesco Romeo,[1,2] Isabella Pallavicini,[1] Sebastiano Peri,[1] Mauro Romanenghi,[1] Juan Alberto Pérez-Valencia,[3,4,5] Eman Hagag,[3,4] Filippo Ferrucci,[3,4,5] Mohamed Elgendy,[3,4,5,6] Orazio Vittorio,[7,8] Salvatore Pece,[1,2] Marco Foiani,[9,2] Jukka Westermarck,[10,11] and Saverio Minucci[1,2,13,*]

[1]Department of Experimental Oncology, IEO IRCCS, Istituto Europeo di Oncologia, Milan, Italy
[2]Department of Oncology and Hemato-Oncology, Università degli Studi di Milano, Milan, Italy
[3]Institute for Clinical Chemistry and Laboratory Medicine, University Hospital and Faculty of Medicine, Technische Universität Dresden, Dresden, Germany
[4]Medical Clinic I, University Hospital Carl Gustav Carus, Technische Universität Dresden, Dresden, Germany
[5]Mildred-Scheel Early Career Center, National Center for Tumor Diseases Dresden (NCT/UCC) University Hospital and Faculty of Medicine, Technische Universität Dresden, Dresden, Germany
[6]Laboratory of Cancer Cell Biology, Institute of Molecular Genetics of the Czech Academy of Sciences, Prague, Czech Republic
[7]Children's Cancer Institute, Lowy Cancer Research Centre, UNSW Sydney, Randwick, NSW, Australia
[8]School of Biomedical Sciences, UNSW Sydney, Randwick, NSW, Australia
[9]IFOM (Fondazione Istituto FIRC di Oncologia Molecolare), Milan, Italy
[10]Turku Bioscience Centre, University of Turku and Åbo Akademi University, Turku, Finland
[11]Institute of Biomedicine, University of Turku, Turku, Finland
[12]Present address: Children's Cancer Institute, Lowy Cancer Research Center, and School of Biomedical Sciences, UNSW Sydney, Randwick, NSW, Australia
[13]Lead contact
*Correspondence: saverio.minucci@ieo.it
https://doi.org/10.1016/j.celrep.2023.112616

SUMMARY

Combined inhibition of oxidative phosphorylation (OXPHOS) and glycolysis has been shown to activate a PP2A-dependent signaling pathway, leading to tumor cell death. Here, we analyze highly selective mitochondrial complex I or III inhibitors *in vitro* and *in vivo* to elucidate the molecular mechanisms leading to cell death following OXPHOS inhibition. We show that IACS-010759 treatment (complex I inhibitor) induces a reactive oxygen species (ROS)-dependent dissociation of CIP2A from PP2A, leading to its destabilization and degradation through chaperone-mediated autophagy. Mitochondrial complex III inhibition has analogous effects. We establish that activation of the PP2A holoenzyme containing B56δ regulatory subunit selectively mediates tumor cell death, while the arrest in proliferation that is observed upon IACS-010759 treatment does not depend on the PP2A-B56δ complex. These studies provide a molecular characterization of the events subsequent to the alteration of critical bioenergetic pathways and help to refine clinical studies aimed to exploit metabolic vulnerabilities of tumor cells.

INTRODUCTION

The altered metabolism of tumor cells has been considered an appealing therapeutic target, although most attempts to develop drugs have been unsuccessful so far.[1–3] As an escape strategy against drugs targeting cellular metabolism, tumor cells in many cases can increase glycolysis when stressed with mitochondrial drugs targeting oxidative phosphorylation (OXPHOS), or increase OXPHOS and oxygen consumption when cultured in low-glucose (LG) condition to impair glycolysis, thus overcoming single inhibition of either pathway.[4–6]

In previous studies, we used metformin as a cellular inhibitor of mitochondrial complex I and therein OXPHOS, for the immediate clinical translatability of our observations, since the drug is widely used in the treatment of type II diabetes and has already been proposed as an anti-cancer drug.[7–9] We discovered that a combination of metformin (to inhibit OXPHOS) and intermittent fasting (to lower glucose levels) leads to activation of a specific signaling cascade mediated by the tumor suppressor Protein Phosphatase 2A (PP2A). PP2A dephosphorylates the serine/threonine kinase GSK3β (which plays a central role in several cellular events) at the inhibitory phosphorylated serine 9, thus increasing its activity. GSK3β activation in turn leads to downregulation of MCL1, an anti-apoptotic member of the BCL2 superfamily, and induction of cell death.[10]

Based on results of this study, we have initiated, in collaboration with other groups, a clinical trial to investigate whether combining metformin with a cyclic fasting-like approach can improve the antitumor activity of neoadjuvant chemotherapy in patients with early-stage triple-negative breast cancer.[11,12] The molecular mechanism of action of metformin, however, remains not definitively established, and different studies have hypothesized a mitochondrial complex I-independent activity for this drug.[13–15]

PP2A consists of three subunits (including several distinct regulatory B subunits, able to direct PP2A toward several substrates).[16,17] Its activity can be inhibited by various endogenous proteins, including CIP2A, which we showed to be downmodulated by metformin treatment.[10] It has been generally observed that a higher level of CIP2A directly correlates with tumor invasiveness, aggressiveness, and bad prognosis.[18] The CIP2A gene promoter is activated in cancer cells by a number of oncogenic mechanisms, including TP53 inhibition and MEK-ERK pathway activation, but recent evidence suggests that CIP2A protein stability is also heavily regulated in cancer at the post-translational level.[19–21] One mechanism leading to CIP2A protein stabilization is its interaction with the B56 subunit of PP2A. However, whether this stabilizing interaction is regulated by signaling mechanisms and what are the molecular events leading to CIP2A protein degradation are very poorly understood. Since CIP2A promotes malignant progression in several cancer types and is associated with resistance of cancer cells to therapies, understanding the post-translational mechanisms regulating CIP2A protein expression is of immediate medical relevance and may provide approaches for therapeutic CIP2A targeting.

To address the molecular mechanisms related to connections between OXPHOS activity, CIP2A expression, and PP2A regulation, we decided to extend our studies to include a recently discovered drug, named IACS-010759, which has proved to be an extremely specific inhibitor of mitochondrial complex I, effective in treatment of OXPHOS-committed tumor cells.[22] IACS-010759, metformin, and other mitochondrial targeting compounds were used in mechanistical studies performed in metabolically plastic tumor cells to answer more precisely the following questions: (1) whether mitochondrial complex I is the actual target for the antitumor effect of the metformin/hypoglycemia treatment, and (2) how inhibition of mitochondrial complex I results in downregulation of CIP2A, which is a required step for PP2A activation.

RESULTS

IACS-010759 targets complex I, and, in combination with LG, activates tumor cell death

IACS-010759 is a potent inhibitor of mitochondrial electron transport chain (ETC) directly binding complex I through its ND1 subunit, and has been previously shown to impair growth of OXPHOS-dependent tumor cells, both *in vitro* and *in vivo*.[22,23] We tested the efficacy of IACS-010759 on HeLa and HCT116 tumor cell lines, which are able to increase their glycolytic rate when challenged with the OXPHOS inhibitor metformin.[10,22] As previously shown, in a short-duration assay (80 min), IACS-010759 weakly affects OXPHOS, unless cells are permeabilized by detergent treatment (Figure S1A), due to its high lipophilicity and a relatively slow cellular uptake.[22] Upon longer exposure, IACS-010759 impairs OXPHOS in both cell lines, which increase their glycolytic rate (Figure S1B). Interestingly, HeLa cells showed a more marked effect than HCT116 on the release of extra-cellular lactate, as an index of glycolytic activity (Figure S1B). HeLa cells adapted to LG with a compensatory increase in oxygen consumption, while HCT116 cells tended to an overall decreased metabolism (Figure S1B). Both HeLa and HCT116 cells showed a modest reduction in growth rate upon metformin treatment, which did not result in an increased cell death (Figure S1C). Consistently, treatment with IACS-010759 resulted in a modest reduction in cell viability, which was more pronounced in HCT116 cells, and absence of cytotoxicity (Figures 1A and S1D). We then tested whether treatment with IACS-010759 in combination with LG levels (which impairs glycolysis) can affect HeLa and HCT116 cell growth and death rate. As observed with metformin, treatment with IACS-010759 in LG strongly reduced cell number compared with high-glucose (HG) conditions (Figure 1A left panel, and S1D left panel). Strikingly, cell death rate upon IACS-010759 dramatically increased in LG, and the effect was dose dependent (Figure 1A right panel, and S1D right panel). Consistently with the switch from a cytostatic to cytotoxic effect of IACS-010759 in LG conditions, while cyclin A levels (as a proliferative marker) were also reduced by the drug in HG conditions, cleaved caspase 3 was detectable only upon treatment in LG-containing medium (Figures 1B and S1E).

To confirm the central role of mitochondrial complex I as a direct target of both IACS-010759-induced growth arrest and cell death, we transduced HCT116 and HeLa cells with viral vectors expressing the yeast complex I orthologue NDI1, which cannot be inhibited by IACS-010759.[22] NDI1-expressing cells show complete resistance to IACS-010759, without reduction in proliferation and almost complete absence of cell death, confirming the role of complex I as the main target of the drug (Figures 1C and S1F). In contrast, overexpression of the NADH oxidase from *Lactobacillus brevis* (Lb)NOX failed to rescue the effect of IACS-010759 in both HeLa and HCT116 cells (Figures S1G and S1H). (Lb)NOX can recycle NAD+ without rescuing the transfer of electrons blocked by IACS-010759, while NDI1 can do both activities; these results therefore point to mitochondrial ETC as a key target of IACS-010759.

Mitochondrial complex I inhibition induces CIP2A downregulation, activating PP2A$^{(B56\delta)}$-GSK3β and leading to MCL1 degradation in LG conditions

In our recent studies, metformin acts by downregulating CIP2A levels, while LG induces a form of the PP2A holoenzyme containing the regulatory subunit B56δ. In turn, PP2A-B56δ activates GSK3β, leading to degradation of MCL1 and apoptosis.[10] As CIP2A functions as a molecular inhibitor of PP2A-B56 complexes, the combined CIP2A inhibition and B56δ induction results in maximal activity of the tumor-suppressive PP2A-B56δ complexes. However, it is unclear which of the numerous molecular target mechanisms of metformin are responsible for CIP2A inhibition and whether complex I inhibition would synergize similarly to metformin with LG. We therefore decided to

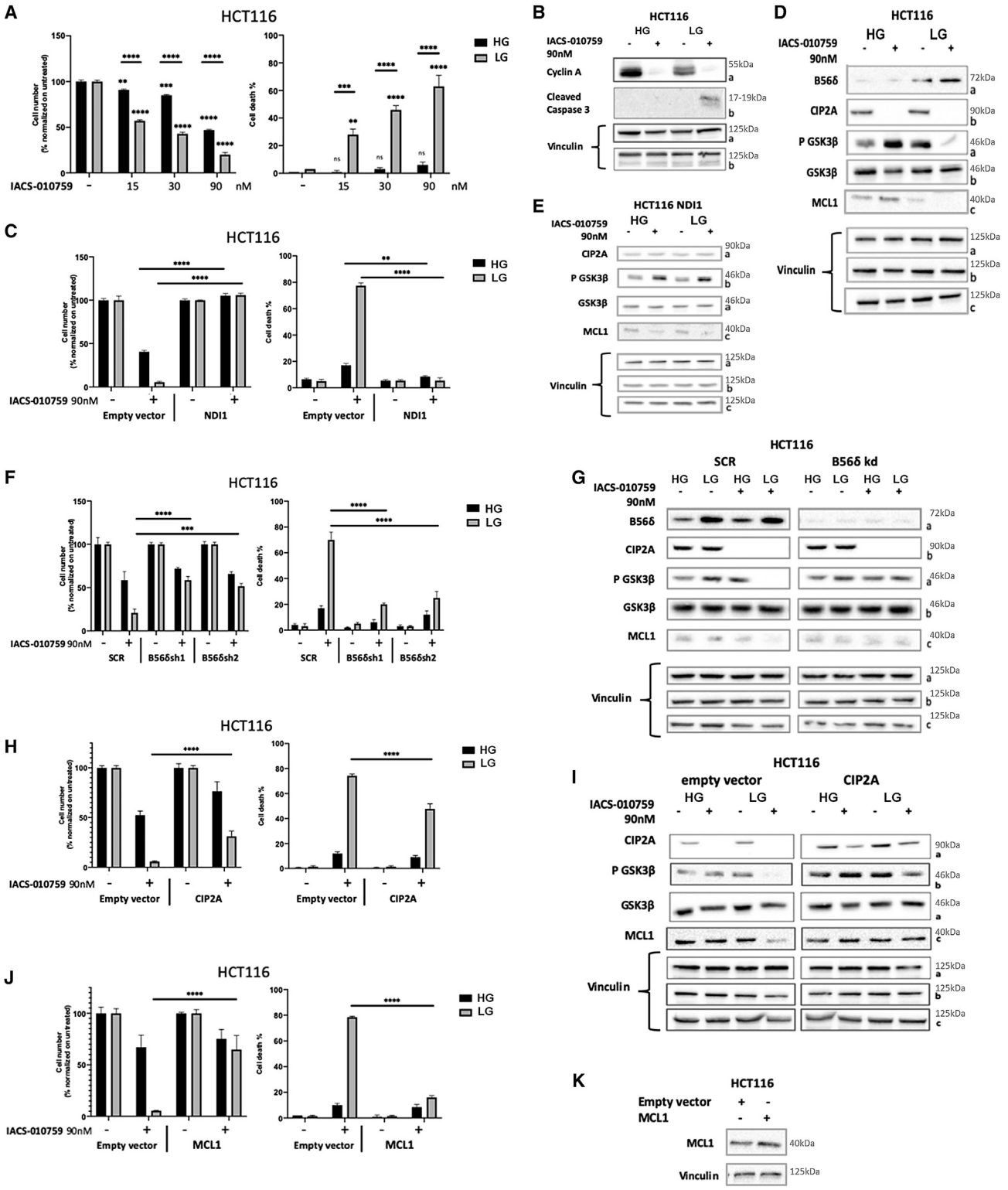

Figure 1. IACS-010759 targets complex I and in LG conditions induces cell death of tumor cells

(A) Proliferation of HCT116 cells cultured either in standard conditions (complete DMEM, 10% fetal bovine serum [FBS], and 10 mM glucose: HG) or in glucose restriction (complete DMEM, 10% FBS, and 2.5 mM glucose: LG). To mimic the *in vivo ad libitum* feeding and/or intermittent fasting cycles in an *in vitro* setting, cells were treated for 24 h in standard conditions, then media were replenished either with standard conditions (*ad libitum* feeding) or glucose starvation

(legend continued on next page)

investigate whether IACS-010579 shares a common molecular mechanism of action with metformin.

As shown in Figures 1D and Figure S1I, IACS-010759 induces (in HeLa and HCT116 cells) a strong downregulation of CIP2A, in both HG and LG conditions. LG treatment per se led to upregulation of the B56δ regulatory subunit, while combination of IACS-10759 and LG activated GSK3β (detected by de-phosphorylation of its Ser9 residue) and induced degradation of MCL1.

Importantly, these molecular events were completely abolished upon overexpression of the yeast complex I orthologue NDI1, showing that the mechanism by which IACS-010759 downregulated CIP2A is mediated by mitochondrial complex I (Figures 1E, and S1L).

To demonstrate that the biological effects of IACS-010759 are mediated by PP2A activation, we knocked down the PP2A-B56δ regulatory subunit in both HeLa and HCT116 cells. Indeed, knockdown of B56δ completely abrogated the increased cell death observed upon IACS-010759 treatment in LG conditions in both HeLa and HCT116 cells (Figures 1F and S2A). Consistently, knockdown of B56δ blocked the downregulation of MCL1 subsequent to GSK3β dephosphorylation upon treatment with metformin in LG conditions in both HeLa and HCT116 cells (Figures 1G and S2B). Interestingly, loss of the B56δ subunit did not rescue the decrease in cell number observed upon IACS-10759 treatment in HG conditions, particularly evident in HCT116 cells (Figure 1F).

We then overexpressed CIP2A in HeLa and HCT116 cells, to attenuate its downregulation induced by IACS-010759. CIP2A overexpression partially rescued the phenotype of IACS-010759 treatment in LG conditions, reducing cell death (Figures 1H and S2C). Modulation of the downstream pathway (GSK3β activation and MCL1 downregulation) was partially rescued by CIP2A overexpression as well (Figures 1I and S2D). Finally, we overexpressed MCL1 to reduce its degradation induced by IACS-010759 in LG conditions. As expected, MCL1 overexpression opposed the dramatic effect of the combination metformin/LG (Figures 1L, 1M, S2E, and S2F). IACS-10759 treatment phenocopied the effect of metformin and similarly triggered in LG conditions a pathway leading to cell death controlled by CIP2A and executed by PP2A-GSK3β-MCL1.

The *in vivo* antitumor effect of IACS-010759 is potentiated by intermittent fasting

Based on the results obtained *in vitro*, we explored the activity of IACS-010759 in murine xenograft models. We treated mice with the drug alone or in combination with intermittent fasting. IACS-010759 administered during *ad libitum* feeding showed a significant reduction in tumor volume. The effect of IACS-010759 was stronger in combination with fasting cycles and was comparable with metformin/fasting (Figures 2A–2C). Mice lost weight during fasting and recovered to normal during feeding cycles (Figure 2D). As shown previously, glycemia dropped during fasting cycles and recovered to normal during feeding[10] (Figure S2G). Consistent with the *in vitro* results, we observed a strong reduction in cyclin A in IACS-010759-treated tumor samples, but cleaved caspase 3 was detectable only in tumor samples from mice treated with IACS-010759 during fasting, indicating that the effect of IACS-010759 was mostly cytostatic in the *ad libitum* feeding group, while the drug was cytotoxic when combined with intermittent fasting (Figure S2H).

Reactive oxygen species induction by metformin and IACS-010759 is required for tumor cell death in LG conditions

We then verified whether complex I inhibition is an obligatory target for the activation of PP2A by targeting mitochondrial complex III with the well-known inhibitor antimycin A. Strikingly, antimycin A treatment in combination with LG resulted in strong

(intermittent fasting) for another 24 h. Cells were treated with increasing concentrations of IACS-010759 as reported in the graphs. Left panels show normalized count of cells, right panels quantification of death by propidium iodide exclusion assay. Data refer to two independent experiments with three replicates each experimental point (n = 6, graph shows mean ± SD).

(B) Immunoblotting analysis of cell lysates derived from (A) for cleaved caspase 3 (as an apoptosis marker) and cyclin A (as a proliferation marker). Vinculin served as a loading control.

(C) Proliferation and survival of HCT116 cells expressing either empty vector as control, or yeast NDI1, treated as in (A). Data refer to two independent experiments with three replicates each experimental point (n = 6, graph shows mean ± SD).

(D) Immunoblot analysis of HCT116 cell lysates, treated as indicated, for CIP2A, the B56δ subunit of PP2A, p-GSK3β (Ser 9) or GSK3β, and MCL1. Vinculin was used as a loading control.

(E) Immunoblot analysis of cell lysates derived from HCT116 cells overexpressing yeast NDI, treated as indicated, for CIP2A, the B56δ subunit of PP2A, p-GSK3β (Ser 9) or GSK3β, and MCL1. Vinculin was used as a loading control. The remaining part of this experiment (control HCT116 cells transfected with the empty vector) can be found in Figure S1L.

(F) Proliferation and survival data of HCT116 cells transduced to express either scrambled short hairpin RNA (shRNA) as a control or two distinct shRNAs targeting the B56δ subunit of PP2A. Cells were grown as described in (A). Left panels show normalized count of cells, right panels quantification of death by propidium iodide exclusion assay. Data refer to two independent experiments with three replicates each experimental point (n = 6, graph shows mean ± SD).

(G) Immunoblotting analysis of cell lysates, derived from experiment in (F), for CIP2A, the B56δ subunit of PP2A, p-GSK3β or GSK3β, and MCL1. Vinculin was used as a loading control.

(H) Proliferation and survival data of HCT116 cells transduced to express CIP2A, or with an empty vector as control, cultured as described in (A). Left panels show normalized count of cells, right panels quantification of death by propidium iodide exclusion assay. Data refer to two independent experiments with three replicates each experimental point (n = 6, graph shows mean ± SD).

(I) Immunoblotting analysis of cell lysates, derived from experiment in (H), for CIP2A, p-GSK3β or GSK3β, and MCL1. Vinculin was used as a loading control.

(J) Proliferation and survival data of HCT116 cells transduced to express MCL1, or with an empty vector as control, cultured as described in (A). Left panels show normalized count of cells, right panels quantification of death by propidium iodide exclusion assay. Data refer to two independent experiments with three replicates each experimental point (n = 6, graph shows mean ± SD).

(K) Immunoblotting analysis of cell lysates derived from experiment in (J), with antibodies against MCL1. Vinculin was used as a loading control, to quantify the amount of MCL1 overexpression (1.44× over control cells).

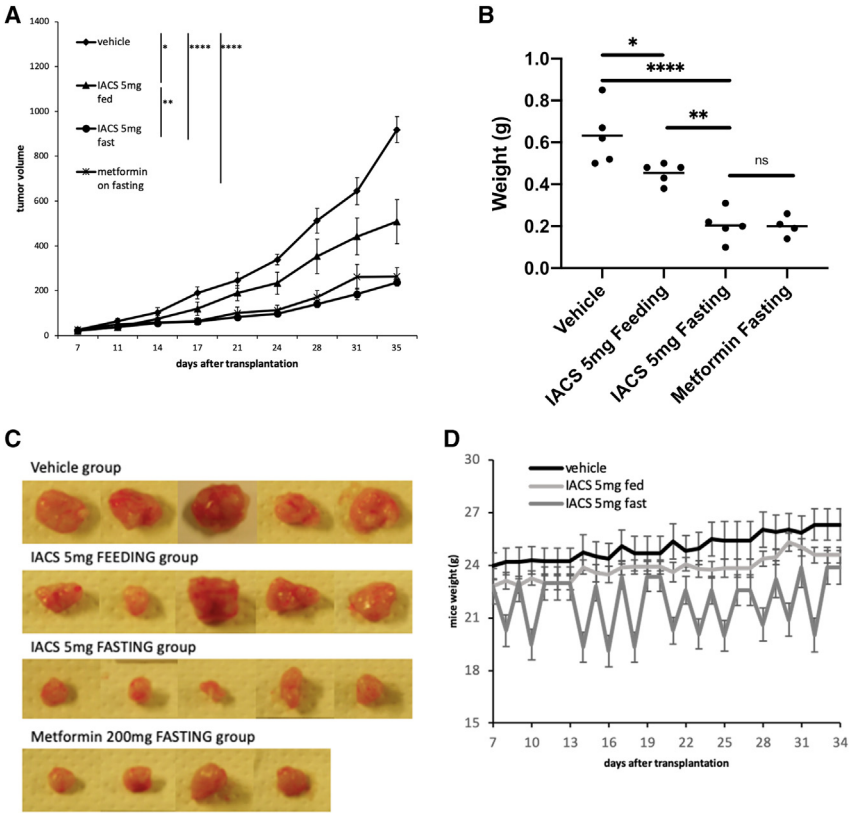

Figure 2. The antitumor effect of IACS-010759 *in vivo* is potentiated by intermittent fasting

CD1 nude mice were inoculated with 5 × 10^6 HCT116 cells. Upon establishment of tumors, mice were randomized in experimental cohorts (five mice each group), IACS-010759 was administered every 24 h (5 mg/kg), metformin every 48 h at higher concentration as in Elgendy et al.[10] (200 mg/kg), feeding groups had free access to food, while fasting groups were kept on 24-h feeding/fasting cycles. We omitted the group treated with intermittent fasting alone, since in our previous study we observed that tumor growth in HCT116 xenografts was not influenced.[10]

(A and B) Growth was measured by (A) tumor volume (mm^3) or (B) tumor weight. Error bars indicate SEM (n = 5 per group). One-way ANOVA test, *p < 0.1; **p < 0.05; ***p < 0.01; ****p < 0.005; ns, non-significant

(C) Images of tumors after surgery.

(D) Mouse weights during treatment (n = 5, graph shows mean ± SD).

lethality in both HeLa and HCT116 cells (Figure S3A). As shown with the mitochondrial complex I inhibitors metformin and IACS-010759, antimycin A was able to downregulate CIP2A protein (Figure S3B).

Metformin and IACS-010759 have been shown to modulate reactive oxygen species (ROS) intracellular content.[15,22,23] Similarly, antimycin A was shown to be a potent ROS inducer.[24,25] Consistently, we observed that both IACS-010759 and antimycin A increased ROS levels in HeLa and HCT116 cells in HG and LG conditions (Figures 3A, S3C, and S3D). Metformin also induced ROS production (Figure S3E). N-acetylcysteine (NAC), commonly used for its antioxidant effect, reduced ROS content to untreated levels (Figure S3E). To more tightly connect ROS production and inhibition of mitochondrial function by the tested drugs, we analyzed ROS production upon treatment by IACS-01079 in the presence of ND1 overexpression, which led to complete abrogation of the drug effect on ROS induction in both HeLa and HCT116 cells (Figure S3F).

We then analyzed mitochondrial morpho-functional parameters and observed signs of mitochondrial dysfunction upon treatment with IACS-010759 already in HG conditions[26–28] (Figures S4A–S4E). Mitochondrial stress was much more evident upon treatment with IACS-010759 in LG conditions, which is consistent with disruption of the mitochondrial network leading to apoptosis.[29–31] In fact, these mitochondrial alterations were rescued by MCL1 overexpression (Figures S4F, S4G).

Given the increased ROS levels observed upon treatment with IACS-010759, metformin, and antimycin A, we investigated the role of ROS as effectors of the action of the drugs. A low-dose concentration of hydrogen peroxide (H_2O_2) (0.5 mM) was sufficient to induce cell death in LG conditions while being relatively unharmful in HG conditions (Figure 3B). Importantly, NAC treatment to restore basal levels of ROS led to a strong reduction in cell death induced by IACS-010759 and metformin in LG conditions, and to an almost complete rescue of the impaired cell growth induced by IACS-010759 in HG conditions (Figures 3C and S5A). We tested other antioxidants, which also restored cell viability with different potency (Figure S5B). Importantly, mito-TEMPO (a selective scavenger of mitochondrial ROS) and S1QEL1 (which suppresses ROS generated by mitochondrial complex I during the process of reverse electron transport) efficiently counteracted the effect of IACS-010759, strongly suggesting that ROS production derives directly from mitochondrial inhibition.[32] Finally, NAC supplemented in drinking water counteracted the antitumor activity of the combination IACS-010759/intermittent fasting *in vivo* (Figure S5C).

ROS induction mediates CIP2A inhibition downstream of complex I inhibition

Mitochondrial complex I inhibition by metformin or IACS-010759 leads to downregulation of CIP2A protein levels, and—as shown above—a shift to glycolysis and an increase in ROS levels. We therefore tried to dissect how these events are mechanistically placed with respect to each other. Knockdown of CIP2A mimics the effect of IACS-010759 in LG conditions, inducing tumor cell death (Figure S6A). Since CIP2A overexpression rescued only partially the effect of IACS-010759 (Figures 1 and S2), this result suggests either technical limitations in the overexpression experiments or additional effects of IACS-010759. CIP2A knockdown, interestingly, failed to modulate tumor cell metabolism

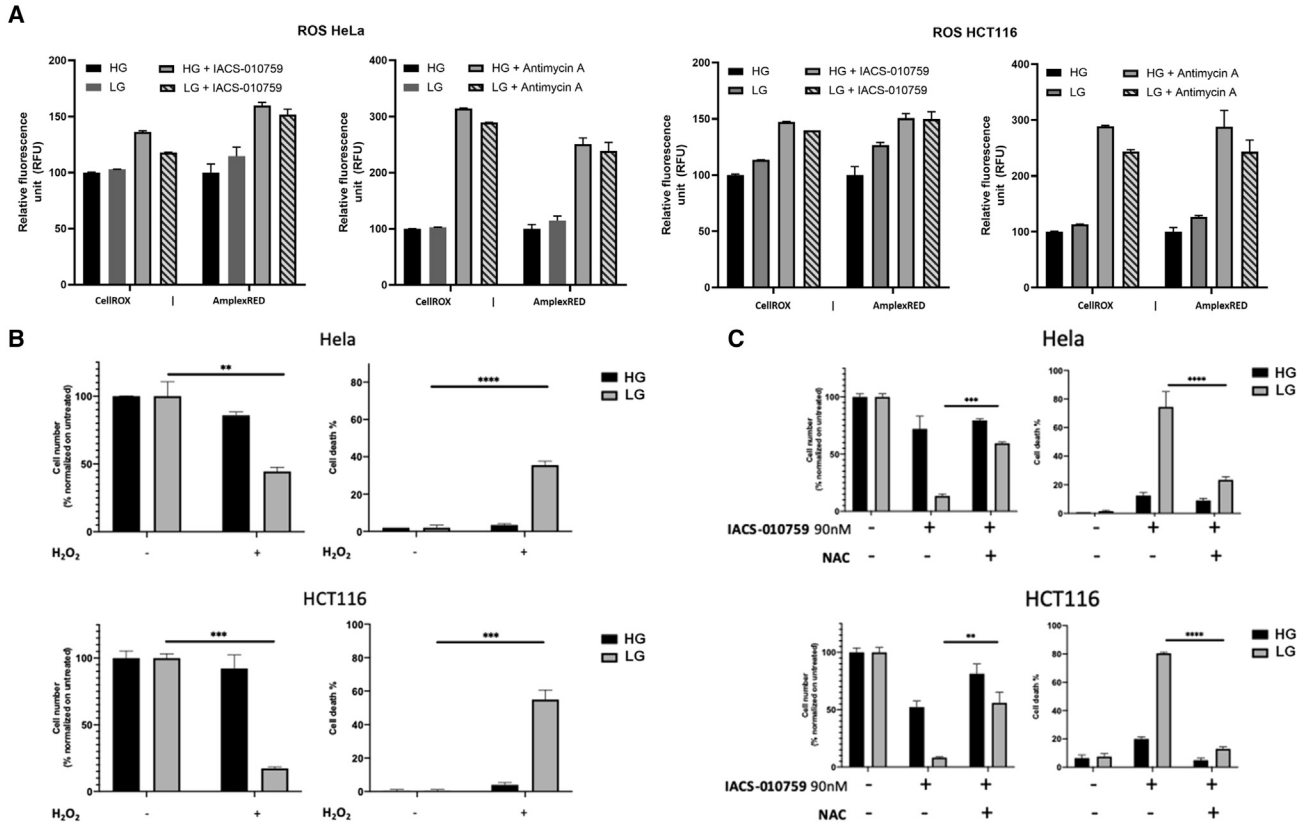

Figure 3. ROS induction is required for tumor cell death in LG conditions

(A) Analysis of ROS levels measured in HeLa and HCT116 cells treated for 36 h with vehicle, IACS-010759, or antimycin A in either HG (10 mM) or LG (2.5 mM) conditions, measured by cellROX (n = 2) or amplexRED (n = 16) assays.

(B) Proliferation and survival data of HeLa and HCT116 cells treated with 0.5 mM H_2O_2 for 24 h, cultured either in standard conditions (10 mM glucose: HG) or in glucose restriction (2.5 mM glucose: LG). Left panels show normalized count of cells, right panels quantification of death by propidium iodide exclusion assay. Data refer to two independent experiments with three replicates each experimental point (n = 6, graph shows mean ± SD).

(C) Proliferation and survival data of HeLa and HCT116 cells cultured 48 h following the protocol described in Figure 1. NAC (5 mM added every 8 h) was added as indicated. Left panels show normalized count of cells, right panels quantification of death by propidium iodide exclusion assay. Data refer to two independent experiments with three replicates each experimental point (n = 6, graph shows mean ± SD).

and ROS levels, as assessed by measuring changes in OCR and ECAR, lactate release, glucose consumption, and ROS induction (Figures S6B–S6F). We hypothesized that altered mitochondrial function occurred upstream of CIP2A downregulation (and therefore it was not observed upon knockdown of CIP2A).

Focusing on ROS induction, we observed that low doses of H_2O_2 (0.5 mM) were sufficient to downmodulate CIP2A protein levels in both HeLa and HCT116 cells (Figure 4A). Consistent with this observation, NAC co-treatment prevented downregulation of CIP2A by IACS-010759 and the activation of $PP2A^{(B56\delta)}$-GSK3β-MCL1 signaling by IACS-010759 in LG conditions (Figures 4B and 4C).

We have shown that downregulation of CIP2A by metformin involves its degradation by the proteasome.[10] Treatment with the proteasome inhibitor MG132, however, led to a modest rescue of CIP2A levels upon treatment of HeLa and HCT116 cells with IACS-010759 (Figure 5A). We hypothesized, therefore, that the proteasome cooperates with additional pathways to regulate CIP2A protein levels. A recent study showed that CIP2A protein stability is regulated by lysosome-mediated degradation.[33] Chaperone-mediated autophagy (CMA) is induced by oxidative stress and by increased Ca^{2+} cytoplasmic levels, and CIP2A has been described as a CMA target in murine cells.[21] Indeed, inhibition of lysosome by chloroquine counteracted downregulation of CIP2A induced by IACS-010759 (Figure 4B). Knockdown of the key CMA component LAMP2A increased basal levels of CIP2A in both HeLa and HCT116 cells (Figures 5A, S7A, and S7B). IACS-010759 treatment downregulated CIP2A protein levels upon LAMP2A knockdown; however, the absolute levels of CIP2A were comparable with those observed under basal conditions in control cells. Likewise, H_2O_2 treatment in the presence of LAMP2A knockdown failed to downmodulate CIP2A protein levels (Figure 5B). The combination of MG132 treatment and LAMP2A knockdown completely rescued CIP2A levels upon IACS-010759 treatment, confirming that the proteasome and CMA cooperate in regulating the stability of CIP2A (Figures 5A, S7A, and S7B). Consistently, knockdown of LAMP2A conferred resistance to IACS-010759 treatment, almost completely

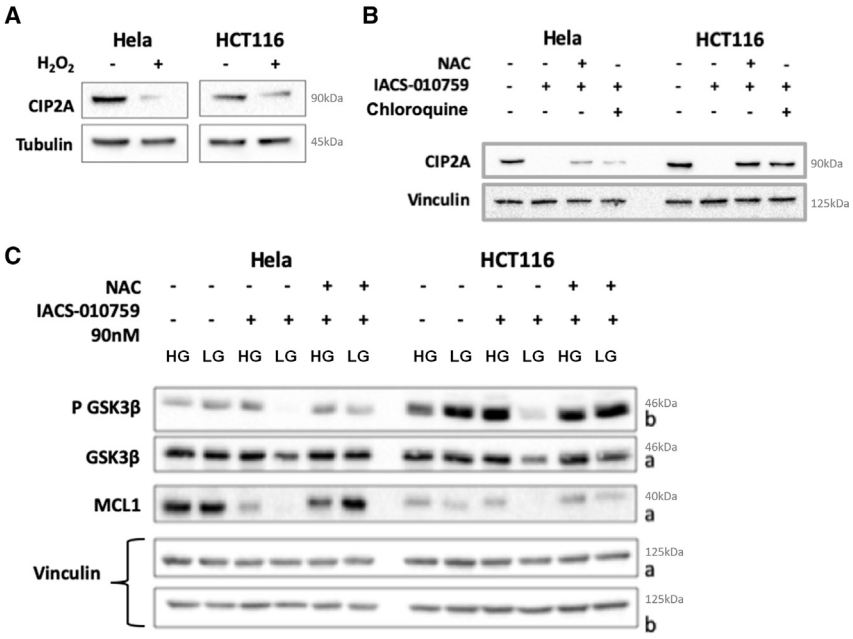

Figure 4. ROS mediate CIP2A downregulation and downstream activation of the PP2A-GSL3β-MCL1 signaling pathway

(A) Immunoblotting analysis to measure CIP2A levels in cell lysates from HeLa and HCT116 cells treated with 0.5mM H_2O_2 for 24 h, cultured in standard conditions. Tubulin was used as a loading control.

(B) Immunoblotting analysis to measure CIP2A levels in cell lysates from HeLa and HCT116 cells treated with IACS-010759 for 48 h, cultured in standard conditions. NAC (5 mM added every 8 h) and chloroquine (20 μM) were added as indicated. Vinculin was used as a loading control.

(C) Immunoblotting analysis to measure levels of p-GSK3β or GSK3β, and of MCL1. Vinculin was used as a loading control. HeLa and HCT116 cells were cultured either in standard conditions (10 mM glucose: HG) or in glucose restriction (2.5 mM glucose: LG). To mimic the *in vivo ad libitum* feeding and/or intermittent fasting cycles in an *in vitro* setting, cells were treated for 24 h in standard conditions, then media were replenished either with standard conditions (HG) or glucose starvation (LG) for other 24 h. NAC (5 mM added every 8 h) was added as indicated.

abrogating cell death in LG conditions in both HeLa and HCT16 cells and increasing viability to levels comparable with NAC treatment in HCT116 cells (Figure 5C).

Protein half-life of CIP2A is regulated by its association with the PP2A B56 regulatory subunit.[34] We therefore tested whether the mutant form of CIP2A previously shown to be compromised in PP2A-B56 association and to be less stable in cancer cells would be subjective to stabilization by lysosomal inhibitor.[34] Indeed, we observed a concentration-dependent rescue of the unstable CIP2A-3A mutant by the lysosomal inhibitor NH_4Cl (Figure S7C). Based on this, we hypothesized that ROS might regulate the association of CIP2A with PP2A required for CIP2A stabilization and that, upon dissociation, CIP2A will be eventually degraded through CMA. We therefore performed a proximity ligation assay (PLA) to detect the association of PP2A (catalytic subunit) and CIP2A, which was readily observed in untreated cells (Figure 6). Addition of IACS-010759 resulted in a strong reduction of the PLA signal, which, however, could be also a consequence of the decreased CIP2A levels (Figure S7D). We performed the same experiment upon knockdown of LAMP2A to allow data interpretation without concomitant CIP2A protein downregulation. Importantly, even under conditions where the stability of CIP2A is maintained, we observed a significant signal decrease in PLA, which was counteracted by NAC addition during treatment with IACS-010759 (Figure 6). Taken together, these results strongly support our hypothesis that IACS-010759, and the following generated ROS, are leading the dissociation of CIP2A from the PP2A complex and its subsequent destabilization and lysosome-related degradation.

DISCUSSION

Using the selective compound IACS-010759 and performing rescue experiments with the yeast ND1 protein, we conclusively define mitochondrial complex I as the critical target of the drug (and of metformin) in triggering the onco-suppressive activation of PP2A in LG conditions, as previously hypothesized by using metformin.[10] We therefore validated our strategy of tackling tumor cells through combinatorial inhibition of oxidative phosphorylation and glycolysis. While several biguanides, other than metformin, are potentially available (including drugs that have been in clinical use, such as phenphormin[35]), we decided to use a completely distinct chemical entity that has been carefully evaluated for its target modulatory activity and that is also in clinical development.[22,23]

The results obtained with the use of IACS-010759 are fully consistent with our model. Achieving a sublethal inhibition of oxidative phosphorylation/glycolysis, which is not sufficient to lead to "metabolic catastrophe" and to a passive mechanism of cell death, tumor cells are able to trigger the biochemical activation of a death-inducing signaling pathway dependent on PP2A activation. Downregulation of the endogenous PP2A inhibitor CIP2A and induction of the B56δ regulatory subunit led to increased amounts of a specific form of the PP2A holoenzyme, which activates GSK3β and in turn leads to degradation of the anti-apoptotic MCL-1 protein, critical for survival. We tested two cell lines (HeLa and HCT116 cells), which show differences in metabolic properties and a different degree of metabolic plasticity, and both showed a similar response to the combination treatment, suggesting that the molecular circuitry that leads to PP2A activation is robust and maintained in different tumor cell contexts.

Notably, in this study we provide additional mechanistical information on the molecular events triggered by inhibition of mitochondrial function by IACS-010759, by metformin itself, and by other mitochondrial targeting compounds.

We observed induction of mitochondrial ROS by treatment with the drugs tested. Previous studies have not consistently

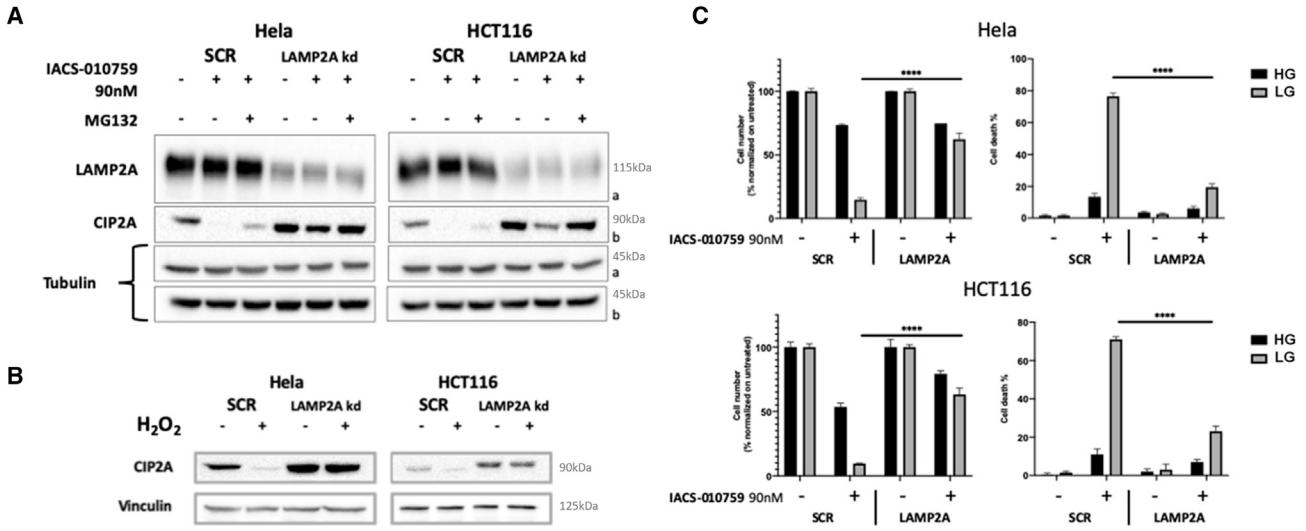

Figure 5. CIP2A degradation, by cooperative action of CMA and the proteasome, mediates the induction of cell death by IACS-010759 in LG conditions

(A) Immunoblotting analysis to measure levels of the indicated proteins, derived from HeLa or HCT116 cells treated as indicated, transduced to express either scrambled shRNA as a control (SCR) or an shRNA targeting LAMP2A. Tubulin was used as a loading control.

(B) Immunoblotting analysis of CIP2A levels from cell lysates derived from HeLa and HCT116 cells treated with 0.5 mM H_2O_2 for 24 h, transduced to express either scrambled shRNA as a control (SCR) or an shRNA targeting LAMP2A.

(C) Proliferation and survival data of HeLa and HCT116 cells, transduced to express either scrambled shRNA as a control (SCR) or shRNAs targeting LAMP2A. Cells were cultured either in standard conditions (10 mM glucose: HG) or in glucose restriction (2.5 mM glucose: LG). To mimic the *in vivo ad libitum* feeding and/or intermittent fasting cycles in an *in vitro* setting, cells were treated for 24 h in standard conditions, then media were replenished either with standard conditions (HG) or glucose starvation (LG) for other 24 h. Left panels show normalized count of cells, right panels quantification of death by propidium iodide exclusion assay. Data refer to two independent experiments with three replicates each experimental point (n = 6, graph shows graph shows mean ± SD).

observed induction of ROS by metformin, but this can be due to properties of the cellular models used and to dose and time of administration of the drug, which may also have additional effects.[36,37] The use of IACS-010759 minimizes these concerns and shows that ROS levels increase in metabolically plastic tumor cells in which mitochondrial complex I function is hampered. Increased ROS production can be ascribed to electron leakage or to retrograde electron transport caused by complex I inhibition.[38,39] The results with the compound S1QEL1, which acts specifically suppressing ROS production during reverse electron transfer, suggest that this may indeed be the target, but more studies are needed to unravel the phenomenon.[40,41]

Our results also show that mitochondrial complex I is not an obligatory target, since we can achieve the same results obtained with metformin or IACS-010759 using drugs such as antimycin A, which targets mitochondrial complex III, leading to ROS production. It appears therefore that the critical event is the generation of ROS by all of these drugs, irrespective of their specific site of action.

Indeed, the increase in ROS production is required for the cytostatic effect of metformin and IACS-010759, observed in the absence of inhibition of glycolysis: NAC addition in HG-containing medium, in fact, completely abrogated the cytostatic effect of the drugs and restored basal ROS levels. Increased ROS levels are also the effectors of the cooperation with LG conditions in triggering PP2A activation. H_2O_2 treatment can mimic the effect of IACS-0101759 (and metformin) in cooperating with LG-containing medium and inducing cytotoxicity, and NAC treatment counteracts the antitumor effect of the combination IACS-010759/intermittent fasting *in vivo*. In addition to NAC, we have used a wide panel of antioxidants that are able to ameliorate cell death induced by IACS-010759 in LG. Specific mitochondrial ROS scavengers, such as mito-TEMPO or S1QEL1, can efficiently rescue the effect of the combination, further confirming mitochondria as a key source of ROS generation.[40]

H_2O_2 treatment is sufficient to downregulate CIP2A levels. In fact, CIP2A is the target for the ROS-mediated effect of the drugs. CIP2A knockdown, while mimicking IACS-010759 or metformin treatment in cooperating with LG conditions, has no effect on cell metabolism per se, and the effect of CIP2A knockdown cannot be rescued by NAC treatment.

Our results also provide mechanistical insights on how the increase in ROS leads to CIP2A downregulation. CIP2A stability is controlled by different pathways, including the proteasome and CMA. CIP2A levels can be stabilized by its inhibitory interaction with the PP2A holoenzyme, and interfering with the CIP2A and PP2A-B56 binding leads to CIP2A proteolytic degradation.[34,42] By knocking down LAMP2A (a critical component of the chaperone-mediated autophagic pathway), we blocked CIP2A degradation and showed conclusively in PLA experiments that the increase in ROS upon IACS-010759 drug treatment leads to dissociation of CIP2A from PP2Ac, and therefore (in the absence of LAMP2A knockdown) to CIP2A degradation. Further studies are required to investigate how ROS trigger dissociation of the complex, but these results provide significant further

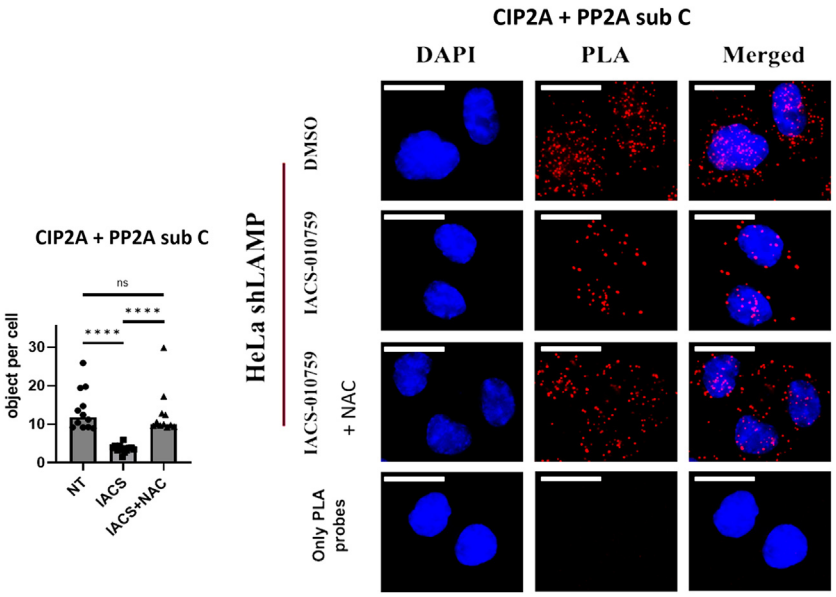

Figure 6. IACS-010759 triggers the ROS-dependent dissociation of CIP2A from PP2A

Proximity ligation assays (PLAs) were performed on LAMP2A knockdown HeLa cells. Cells were either treated with vehicle (DMSO), or treated with IACS-010759 90 nM, or treated with IACS-010759 90 nM plus NAC (5 mM added every 8 h). Left panel shows the quantification of PLA dots (1 dot = 1 interaction between CIP2A and PP2A subunit C). ****$p < 0.005$; ns, non-significant. Panels on the right show representative images of DAPI-stained nuclei, PLA reactions, and merged signals. Bottom row (only PLA probes) shows a control with PLA probes only. Data are representative of two independent experiments with 10 acquisitions over each experimental point (n = 20, mean and values). Scale bar, 10 μm.

understanding of how protein stability of one of the most prevalent human oncoproteins across human cancers is regulated.

Our studies also show that the activation of the PP2A$^{B56\delta}$ holoenzyme is required to trigger the cytotoxic effect of the combination of IACS-010759/LG but not the cytostatic effect induced by IACS-010759 treatment alone. While NAC treatment can counteract both phenomena, knockdown of the B56δ B-regulatory PP2A subunit is able to block cytotoxicity, while it does not prevent the arrest in cell proliferation. Finally, the molecular events following PP2A-B56δ activation led to profound effects on morpho-functional mitochondrial parameters: strikingly, forced expression of MCL1 is able to completely block these mitochondrial alterations, abrogating cell death.

The use of metformin in millions of diabetic patients has shown the relative safety of drugs inhibiting mitochondrial function, with promising clinical data in specific contexts, such as patients with advanced pancreatic neuroendocrine tumors.[43] There are, however, several issues related to the actual mechanisms and the degree of OXPHOS inhibition observed in patients. The interpretation of several preclinical studies has been questioned, given the high doses of metformin used compared with those that can be reached in most tissues upon clinical administration of the drug.[7,9,44]

Here, we have tried to bypass these issues by using a different drug that acts as a much more potent and selective drug than metformin on mitochondrial complex I, being already maximally active at nanomolar concentrations (at least two logs less than metformin). Indeed, IACS-010759 treatment of both cellular and animal tumor models confirmed the finding that mitochondrial complex I is the key target and its inhibition the main effector mechanism for the biological response that we observed.

With the remarkable exception of metformin, clinical results with OXPHOS inhibitors have not shown a convenient safety profile. The clinical efficacy of this strategy, additionally, has recently been questioned even for metformin.[45] Here, our studies suggest that combinatorial treatments with dietary regimens able to significantly reduce glycemic levels could trigger novel biochemical pathways (PP2A(B56δ)/GSK3β/MCL1) and perhaps enhance the safety profile of OXPHOS inhibitors (including IACS-010759) toward a more manageable state. Those dietary regimens are indeed being tested in clinical trials[11,46] and will show the clinical feasibility of our approach and its efficacy in the clinical setting.

Limitations of the study

We used throughout our study cell lines, and we did not explore primary cells, which may show different metabolic properties. We tend to consider this unlikely, since we made extensive use of melanoma primary cells in one previous study, with comparable results.[10] Additionally, the *in vivo* studies are based on murine xenograft models, to allow engraftment of the human tumor cells. We therefore did not explore the contribution of the immune system and the response of the immune system to the tested treatments. We are currently pursuing studies to address this point.

STAR★METHODS

Detailed methods are provided in the online version of this paper and include the following:

- KEY RESOURCES TABLE
- RESOURCE AVAILABILITY
  - Lead contact
  - Materials availability
  - Data and code availability
- EXPERIMENTAL MODEL AND STUDY PARTICIPANT DETAILS
  - Cell lines
  - Xenograft tumor models
- METHOD DETAILS
  - *In vitro* treatment of cells in high and low glucose conditions
  - Knockdown and overexpression experiments
  - Immunoblotting
  - Immunofluorescence
  - Proximity ligation assay (PLA)

SUPPLEMENTAL INFORMATION

Supplemental information can be found online at https://doi.org/10.1016/j.celrep.2023.112616.

ACKNOWLEDGMENTS

This work was partially supported by the Italian Ministry of Health with Ricerca Corrente and 5x1000 funds. S.M. is funded by AIRC (IG20-24944). J.W. was funded by Sigrid Juselius Foundation. M.E. has received funding from the European Research Council (ERC) under Horizon 2020 research and innovation programme (Onco-Energetics_OFF, grant agreement no. 852761) and has received partial support from Czech Science Foundation (project no. 19-22156Y) and National Institute for Cancer Research (Program EXCELES, ID project no. LX22NPO5102).

We would like to thank the Therapeutics Discovery Division at The University of Texas MD Anderson Cancer Center, particularly Giulio Draetta and Christopher Vellano, for providing IACS-010759; Isabella Dalle Donne and Graziano Colombo (University of Milan) for experimental support and comments; and Bruno Amati, Giulio Donati (European Institute of Oncology, Milan), Claudio Vernieri (IFOM and National Cancer Institute, Milan), and Marco Giorgio (University of Padua) for their useful insights, comments, and scientific discussion. Graphical abstract created with BioRender.com

AUTHOR CONTRIBUTIONS

Conceptualization, R.C. and S.M.; methodology, R.C., F.R., and S.M.; investigation, R.C., F.R., I.P., S. Peri, M.R., J.P.-V., E.H., and F.F.; writing – original draft, R.C. and S.M.; writing – review & editing, M.E., O.V., S. Pece, M.F., and J.W.; funding acquisition, S.M. and M.E.; supervision, S.M.

DECLARATION OF INTERESTS

The authors declare no competing interests.

INCLUSION AND DIVERSITY

We support inclusive, diverse, and equitable conduct of research.

Received: August 9, 2022
Revised: April 15, 2023
Accepted: May 23, 2023
Published: June 7, 2023

REFERENCES

1. Jose, C., Bellance, N., and Rossignol, R. (2011). Choosing between glycolysis and oxidative phosphorylation: a tumor's dilemma? Biochim. Biophys. Acta - Bioenerg., 552–561.
2. DeBerardinis, R.J., and Chandel, N.S. (2020). We need to talk about the Warburg effect. Nat Metab *2*, 127–129. https://doi.org/10.1038/s42255-020-0172-2.
3. Martinez-Outschoorn, U., Peiris-Pagés, M., and Pestell, R. (2017). Cancer metabolism: a therapeutic perspective. Nat. Rev. Clin. Oncol. *14*, 11–31. https://doi.org/10.1038/nrclinonc.2016.60.
4. Jia, D., Lu, M., Jung, K.H., Park, J.H., Yu, L., Onuchic, J.N., Kaipparettu, B.A., and Levine, H. (2019). Elucidating cancer metabolic plasticity by coupling gene regulation with metabolic pathways. Proc. Natl. Acad. Sci. USA *116*, 3909–3918. https://doi.org/10.1073/pnas.1816391116.
5. Biancur, D.E., and Kimmelman, A.C. (2018). The plasticity of pancreatic cancer metabolism in tumor progression and therapeutic resistance. Biochim. Biophys. Acta Rev. Canc *1870*, 67–75. https://doi.org/10.1016/j.bbcan.2018.04.011.
6. Ganapathy-Kanniappan, S. (2018). Turning cancer's metabolic plasticity into fragility- an evolving paradigm. Cancer Biol. Ther. *19*, 763–765. https://doi.org/10.1080/15384047.2018.1471441.
7. Hong, Y., Xi, Z., Peng, G., Jinxin, S., Zhonghua, W., Zhexu, G., Zhenning, W., and Yongxi, S. (2019). The potential effect of metformin on cancer: an umbrella review. Front. Endocrinol. https://doi.org/10.3389/fendo.2019.00617.
8. Sehdev, A., Shih, Y.T., Vekhter, B., Bissonnette, M.B., Olopade, O.I., and Polite, B.N. (2015). Metformin for primary colorectal cancer prevention in patients with diabetes: a case-control study in a US population. Cancer *121*, 1071–1078. https://doi.org/10.1002/cncr.29165.
9. Wheaton WW, Weinberg SE, Hamanaka RB, Soberanes S, Sullivan LB, Anso E, Glasauer A, Dofour E, Mutlu GM, Budigner GRS and Chandel NS (2014). Metformin inhibits mitochondrial complex I of cancer cells to reduce tumorigenesis. Elife. https://doi.org/10.7554/eLife.02242.001.
10. Elgendy M, Cirò M, Hosseini A, Weiszmann J, Mazzarella L, Ferrari E, Cazzoli R, Curigliano G, DeCensi A, Bonanni B, et al. (2019) Combination of hypoglycemia and metformin impairs tumor metabolic plasticity and growth by modulating the PP2A-GSK3β-MCL-1 Axis. Cancer Cell. 2019 May 13;35:798-815.e5. https://doi.org/10.1016/j.ccell.2019.03.007.
11. Vernieri, C., Fucà, G., Ligorio, F., Huber, V., Vingiani, A., Iannelli, F., Raimondi, A., Rinchai, D., Frigè, G., Belfiore, A., et al. (2022). Fasting-mimicking diet is safe and reshapes metabolism and antitumor immunity in patients with cancer. Cancer Discov. *12*, 90–107. https://doi.org/10.1158/2159-8290.CD-21-0030.
12. Fondazione IRCCS Istituto Nazionale dei Tumori (2022). Calorie restriction with or without metformin in triple negative breast cancer (BREAKFAST) (Milan).
13. Di Magno, L., Manni, S., Di Pastena, F., Coni, S., Macone, A., Cairoli, S., Sambucci, M., Infante, P., Moretti, M., Petroni, M., et al. (2020). Phenformin inhibits hedgehog-dependent tumor growth through a complex I-independent redox/corepressor module. Cell Rep. *30*, 1735–1752.e7. https://doi.org/10.1016/j.celrep.2020.01.024. PMID: 32049007.
14. Madiraju, A.K., Erion, D.M., Rahimi, Y., Zhang, X.M., Braddock, D.T., Albright, R.A., Prigaro, B.J., Wood, J.L., Bhanot, S., and MacDonald, M.J. (2014). Metformin suppresses gluconeogenesis by inhibiting mitochondrial glycerophosphate dehydrogenase. Nature *510*, 542–546.
15. Khan, H., Anshu, A., Prasad, A., Roy, S., Jeffery, J., Kittipongdaja, W., Yang, D.T., and Schieke, S.M. (2019). Metabolic rewiring in response to biguanides is mediated by mROS/HIF-1a in malignant lymphocytes. Cell Rep. *29*, 3009–3018.e4. https://doi.org/10.1016/j.celrep.2019.11.007. PMID: 31801069.
16. Westermarck, J., and Hahn, W.C. (2008). Multiple pathways regulated by the tumor suppressor PP2A in transformation. Trends Mol. Med. *14*, 152–160. https://doi.org/10.1016/j.molmed.2008.02.001.
17. Shi, Y. (2009). Serine/threonine phosphatases: mechanism through structure. Cell *139*, 468–484. https://doi.org/10.1016/j.cell.2009.10.006.
18. Tang, M., Shen, J.-F., Li, P., Zhou, L.-N., Zeng, P., and Cui, X.-X. (2018). Prognostic significance of CIP2A expression in solid tumors: a meta-analysis. PLoS One *13*, e0199675. https://doi.org/10.1371/journal.pone.0199675.
19. Junttila, M.R., Puustinen, P., Niemelä, M., Ahola, R., Arnold, H., Böttzauw, T., Ala-aho, R., Nielsen, C., Ivaska, J., Taya, Y., et al. (2007). CIP2A inhibits PP2A in human malignancies. Cell *130*, 51–62. https://doi.org/10.1016/j.cell.2007.04.044.
20. Puustinen, P., Rytter, A., Mortensen, M., Kohonen, P., Moreira, J.M., and Jäättelä, M. (2014). CIP2A oncoprotein controls cell growth and autophagy through mTORC1 activation. J. Cell Biol. *204*, 713–727. https://doi.org/10.1083/jcb.201304012.
21. Gomes, L.R., Menck, C.F.M., and Cuervo, A.M. (2017). Chaperone-mediated autophagy prevents cellular transformation by regulating MYC

proteasomal degradation. Autophagy *13*, 928–940. https://doi.org/10.1080/15548627.2017.1293767.

22. Molina, J.R., Sun, Y., Protopopova, M., Gera, S., Bandi, M., Bristow, C., McAfoos, T., Morlacchi, P., Ackroyd, J., Agip, A.A., et al. (2018). An inhibitor of oxidative phosphorylation exploits cancer vulnerability. Nat. Med. *24*, 1036–1046. https://doi.org/10.1038/s41591-018-0052-4.
23. Tsuji, A., Akao, T., Masuya, T., Murai, M., and Miyoshi, H. (2020). IACS-010759, a potent inhibitor of glycolysis-deficient hypoxic tumor cells, inhibits mitochondrial respiratory complex I through a unique mechanism. J. Biol. Chem. *295*, 7481–7491. https://doi.org/10.1074/jbc.RA120.013366.
24. Pecinova, A., Drahota, Z., Kovalcikova, J., Kovarova, N., Pecina, P., Alan, L., Zima, M., Houstek, J., and Mracek, T. (2017). Pleiotropic effects of biguanides on mitochondrial reactive oxygen species production. Oxid. Med. Cell. Longev. https://doi.org/10.1155/2017/7038603.
25. Park, W.H., Han, Y.W., Kim, S.H., and Kim, S.Z. (2007). An ROS generator, antimycin A, inhibits the growth of HeLa cells via apoptosis. J. Cell. Biochem. *102*, 98–109. https://doi.org/10.1002/jcb.21280.
26. Zorov, D.B., Juhaszova, M., and Sollott, S.J. (2014). Mitochondrial reactive oxygen species (ROS) and ROS-induced ROS release. Physiol. Rev. *94*, 909–950. https://doi.org/10.1152/physrev.00026.2013.
27. Poburko, D., and Demaurex, N. (2012). Regulation of the mitochondrial proton gradient by cytosolic Ca^{2+} signals. Pflügers Archiv *464*, 19–26. https://doi.org/10.1007/s00424-012-1106-y.
28. Van de Water, B., Zoeteweij, J.P., de Bont, H.J., Mulder, G.J., and Nagelkerke, J.F. (1994). Role of mitochondrial Ca^{2+} in the oxidative stress-induced dissipation of the mitochondrial membrane potential. Studies in isolated proximal tubular cells using the nephrotoxin 1,2-dichlorovinyl-L-cysteine. J. Biol. Chem. *269*, 14546–14552.
29. Tondera, D., Grandemange, S., Jourdain, A., Karbowski, M., Mattenberger, Y., Herzig, S., Da Cruz, S., Clerc, P., Raschke, I., Merkwirth, C., et al. (2009). SLP-2 is required for stress-induced mitochondrial hyperfusion. EMBO J. *28*, 1589–1600. https://doi.org/10.1038/emboj.2009.89.
30. Ohshima, Y., Takata, N., Suzuki-Karasaki, M., Yoshida, Y., Tokuhashi, Y., and Suzuki-Karasaki, Y. (2017). Disrupting mitochondrial Ca^{2+} homeostasis causes tumor-selective TRAIL sensitization through mitochondrial network abnormalities. Int. J. Oncol. *51*, 1146–1158. https://doi.org/10.3892/ijo.2017.4096.
31. Shutt, T.E., and McBride, H.M. (2012). Staying cool in difficult times: mitochondrial dynamics, quality control and the stress response. Biochim. Biophys. Acta *1833*, 417–424. https://doi.org/10.1016/j.bbamcr.2012.05.024.
32. Orr, A.L., Vargas, L., Turk, C.N., Baaten, J.E., Matzen, J.T., Dardov, V.J., Attle, S.J., Li, J., Quackenbush, D.C., Goncalves, R.L.S., et al. (2015). Suppressors of superoxide production from mitochondrial complex III. Nat. Chem. Biol. *11*. https://doi.org/10.1038/nchembio.1910.
33. Puustinen, P., and Jäättelä, M. (2014). KIAA1524/CIP2A promotes cancer growth by coordinating the activities of MTORC1 and MYC. Autophagy *10*, 1352–1354. https://doi.org/10.4161/auto.29076.
34. Wang, J., Okkeri, J., Pavic, K., Wang, Z., Kauko, O., Halonen, T., Sarek, G., Ojala, P.M., Rao, Z., Xu, W., and Westermarck, J. (2017). Oncoprotein CIP2A is stabilized via interaction with tumor suppressor PP2A/B56. EMBO Rep. *18*, 437–450. https://doi.org/10.15252/embr.201642788.
35. Geoghegan, F., Chadderton, N., Farrar, G.J., Zisterer, D.M., and Porter, R.K. (2017). Direct effects of phenformin on metabolism/bioenergetics and viability of SH-SY5Y neuroblastoma cells. Oncol. Lett. *14*, 6298–6306. https://doi.org/10.3892/ol.2017.6929.
36. Warkad, M.S., Kim, C.H., and Kang, B.G. (2021). Metformin-induced ROS upregulation as amplified by apigenin causes profound anticancer activity while sparing normal cells. Sci. Rep. *11*, 14002. https://doi.org/10.1038/s41598-021-93270-0.
37. Algire, C., Moiseeva, O., Deschênes-Simard, X., Amrein, L., Petruccelli, L., Birman, E., Viollet, B., Ferbeyre, G., and Pollak, M.N. (2012). Metformin reduces endogenous reactive oxygen species and associated DNA damage. Cancer Prev. Res. *5*, 536–543. https://doi.org/10.1158/1940-6207.CAPR-11-0536.
38. Zorov, D.B., Juhaszova, M., and Sollott, S.J. (2006). Mitochondrial ROS-induced ROS release: an update and review. Biochim. Biophys. Acta *1757*, 509–517. https://doi.org/10.1016/j.bbabio.2006.04.029.
39. Dunn, J.D., Alvarez, L.A., Zhang, X., and Soldati, T. (2015). Reactive oxygen species and mitochondria: a nexus of cellular homeostasis. Redox Biol. *6*, 472–485. https://doi.org/10.1016/j.redox.2015.09.005.
40. Kong, H., Reczek, C.R., McElroy, G.S., Steinert, E.M., Wang, T., Sabatini, D.M., and Chandel, N.S. (2020). Metabolic determinants of cellular fitness dependent on mitochondrial reactive oxygen species. Sci. Adv. *6*.
41. Brand, M.D., Goncalves, R.L.S., Orr, A.L., Vargas, L., Gerencser, A.A., Borch Jensen, M., Wang, Y.T., Melov, S., Turk, C.N., Matzen, J.T., et al. (2016). Suppressors of superoxide-H2O2 production at site IQ of mitochondrial complex I protect against stem cell hyperplasia and ischemia-reperfusion injury. Cell Metabol. *24*, 582–592. https://doi.org/10.1016/j.cmet.2016.08.012.
42. Pavic, K., Gupta, N., Omella, J.D., Derua, R., Aakula, A., Huhtaniemi, R., Määttä, J.A., Höfflin, N., Okkeri, J., Wang, Z., et al. (2023). Structural mechanism for inhibition of PP2A-B56α and oncogenicity by CIP2A. Nat. Commun. *14*, 1143. https://doi.org/10.1038/s41467-023-36693-9.
43. Pusceddu, S., Vernieri, C., Di Maio, M., Marconcini, R., Spada, F., Massironi, S., Ibrahim, T., Brizzi, M.P., Campana, D., Faggiano, A., et al. (2018). Metformin use is associated with longer progression-free survival of patients with diabetes and pancreatic neuroendocrine tumors receiving everolimus and/or somatostatin analogues. Gastroenterology *155*, 479–489.e7. https://doi.org/10.1053/j.gastro.2018.04.010.
44. Chandel, N.S., Avizonis, D., Reczek, C.R., Weinberg, S.E., Menz, S., Neuhaus, R., Christian, S., Haegebarth, A., Algire, C., and Pollak, M. (2016). Are metformin doses used in murine cancer models clinically relevant? Cell Metabol. *23*, 569–570. https://doi.org/10.1016/j.cmet.2016.03.010.
45. Goodwin, P.J., Chen, B.E., Gelmon, K.A., Whelan, T.J., Ennis, M., Lemieux, J., Ligibel, J.A., Hershman, D.L., Mayer, I.A., Hobday, T.J., et al. (2022). Effect of metformin vs placebo on invasive disease–free survival in patients with breast cancer. JAMA *327*, 1963–1973. https://doi.org/10.1001/jama.2022.6147.
46. Caffa, I., Spagnolo, V., Vernieri, C., Valdemarin, F., Becherini, P., Wei, M., Brandhorst, S., Zucal, C., Driehuis, E., Ferrando, L., et al. (2020). Fasting-mimicking diet and hormone therapy induce breast cancer regression. Nature, 1–29. https://doi.org/10.1038/s41586-020-2502-7.
47. Titov, D.V., Cracan, V., Goodman, R.P., Peng, J., Grabarek, Z., and Mootha, V.K. (2016). Complementation of mitochondrial electron transport chain by manipulation of the NAD+/NADH ratio. Science *352*, 231–235. https://doi.org/10.1126/science.aad4017.
48. Stewart, S.A., Dykxhoorn, D.M., Palliser, D., Mizuno, H., Yu, E.Y., An, D.S., Sabatini, D.M., Chen, I.S., Hahn, W.C., Sharp, P.A., et al. (2003). Lentivirus-delivered stable gene silencing by RNAi in primary cells. RNA *9*, 493–501. https://doi.org/10.1261/rna.2192803.
49. Akama-Garren, E., Joshi, N., Tammela, T., Chang, G.P., Wagner, B.L., Lee, D.Y., Rideout Iii, W.M., Papagiannakopoulos, T., Xue, W., Jacks, T., et al. (2016). A modular assembly platform for rapid generation of DNA constructs. Sci. Rep. *6*, 16836. https://doi.org/10.1038/srep16836.
50. Schneider CA, Rasband WS, Eliceiri KW. NIH Image to ImageJ: 25 years of image analysis. Nat. Methods. 2012 Jul;9:671-675. doi: 10.1038/nmeth.2089.

STAR★METHODS

KEY RESOURCES TABLE

REAGENT or RESOURCE	SOURCE	IDENTIFIER
Antibodies		
Phospho-GSK-3β (Ser9) rabbit pAb	Cell Signaling Technology	Cat#9336; RRID: AB_331405
GSK-3β (27C10) Rabbit mAb	Cell Signaling Technology	Cat#9315; RRID: AB_490890
Cleaved Caspase-3 (Asp175) (5A1E) Rabbit mAb	Cell Signaling Technology	Cat#9664; RRID: AB_2070042
Vinculin (7F9) mouse mAb	Santa Cruz Biotechnology	Cat#sc-73614; RRID: AB_1131294
Mcl-1 (D35A5) Rabbit mAb	Cell Signaling Technology	Cat#5453; RRID: AB_10694494
Tubulin (TU-02) mouse mAb	Santa Cruz Biotechnology	Cat#sc-8035; RRID: AB_628408
Cyclin A (BF683) mouse mAb	Santa Cruz Biotechnology	Cat#sc-239; RRID: AB_627334
PP2A subunit B56δ (H5D12) mouse mAb	Santa Cruz Biotechnology	Cat#sc-81605; RRID: AB_2168125
LAMP-2 (H4B4) mouse mAb	Santa Cruz Biotechnology	Cat#sc-18822; RRID: AB_626858
CIP2A (HL1925) mouse mAb	Santa Cruz Biotechnology	Cat#sc-80662; RRID: AB_2130800
Tom20 (F-10) mouse mAb	Santa Cruz Biotechnology	Cat#sc-17764; RRID: AB_628381
Actin (AC-40) mouse mAb	Sigma Aldrich	Cat#A4700; RRID: AB_476730
FLAG tag (M2) mouse mAb	Sigma Aldrich	Cat#F1804; RRID: AB_262044
PP2A subunit C clone 1D6 mouse mAb	Merck	Cat#05–421; RRID: AB_309726
CIP2A rabbit pAb	Millipore/Sigma	Cat#ABC307
Bacterial and virus strains		
pLenti6.3_GFP	Invitrogen	Cat# V53306 RRID: Addgene_104402
pUC57-LbNOX	Titov et al. Science. 2016[47]	Addgene plasmid #75285 RRID: Addgene_75285
pLKO.1-puro	Stewart et al. RNA 2003[48]	Addgene plasmid #8453 RRID: Addgene_8453
pLVX-puro	Clontech	Cat# PVT2301 RRID: Addgene_125839
MSVC-puro	Akama-Garren et al. Sci Rep. 2016[49]	Addgene plasmid #68469 RRID: Addgene_68469
Chemicals, peptides, and recombinant proteins		
IACS-010957	Molina et al.[22]	University of Texas MD Anderson Cancer Center under MTA
Metformin	Sigma-Aldrich	D150959; CAS: 1115-70-4
Antimycin A	Sigma-Aldrich	A8674; CAS: 1397-94-0
S1QEL1	Sigma-Aldrich	SML1948; CAS: 897613-29-5
S3QEL2	Sigma-Aldrich	SML1554; CAS: 890888-12-7
α-Tocopherol	Sigma-Aldrich	258024; CAS: 10191-41-0
(S)-Trolox methyl ether	Sigma-Aldrich	93510; CAS:135806-59-6
N-Acetyl-L-cysteine	Sigma-Aldrich	A7250; CAS: 616-91-1
MitoTEMPO	Sigma-Aldrich	SML0737; CAS:1334850-99-5 1334850-99-5
N-Acetyl-L-cysteine ethyl ester	Sigma-Aldrich	01042; CAS: 7652-46-2
Critical commercial assays		
Extracellular lactate Detection Kit	Thermofisher	NEG772014MC
Glucose Colorimetric Detection Kit	Thermofisher	EIAGLUC

(*Continued on next page*)

Continued

REAGENT or RESOURCE	SOURCE	IDENTIFIER
Fura-2, AM, cell permeant	Invitrogen	F1221
CellROX™ Deep Red Reagent	Thermofisher	C10422
Amplex™ Red Reagent	Thermofisher	A12222
Duo-link PLA kit	Sigma-Aldrich	DUO92101
Experimental models: Cell lines		
Human: HeLa cell line	ATCC	ATCC CRM-CCL-2
Human: HCT116 cell line	ATCC	ATCC CCL-247EMT
Experimental models: Organisms/strains		
Mouse: CD1 nude mice Crl:CD1-Foxn1nu Immunodeficient	Charles River	strain 086
Oligonucleotides		
shRNA targeting sequence: CIP2A FW1: CCGGTGCGGCACTTGGAGGTA ATTTCTCGAGAAATTACCTCCAA GTGCCGCATTTTTG CIP2A RV1: AATTCAAAAATGCGGCACTTGGA GGTAATTTCTCGAGAAATTACCTC CAAGTGCCGCA	This paper	N/A
shRNA targeting sequence: CIP2A FW2: CCGGATTTGTGACTTCGTAACAAT ACTCGAGTATTGTTACGAAGTCAC AAATTTTTTG CIP2A RV2: AATTCAAAAAATTTGTGACTTCGT AACAATACTCGAGTATTGTTACGA AGTCACAAAT	This paper	N/A
shRNA targeting sequence: B56δ FW1: CCGGCACATCTCCAGCTCGTGT ATGCTCGAGCATACACGAGCTG GAGATGTGTTTTTG B56δ RV1: AATTCAAAAACACATCTCCAGCT CGTGTATGCTCGAGCATACACG AGCTGGAGATGTG	This paper	N/A
shRNA targeting sequence: B56δ FW2: CCGGAGTCTGACTGAGCCGGT AATTCTCGAGAATTACCGGCTC AGTCAGACTTTTTTG B56δ RV2: AATTCAAAAAAGTCTGACTGAGC CGGTAATTCTCGAGAATTACCGG CTCAGTCAGACT	This paper	N/A
shRNA targeting sequence: LAMP2A FW1: CCGGGTACGCTATGAAACTAC AAATCTCGAGATTTGTAGTTTC ATAGCGTACTTTTTG LAMP2A RV1: AATTCAAAAAGTACGCTATGAA ACTACAAATCTCGAGATTTGTA GTTTCATAGCGTAC	This paper	N/A

(*Continued on next page*)

Continued

REAGENT or RESOURCE	SOURCE	IDENTIFIER
shRNA targeting sequence: LAMP2A FW2: CCGGGCCATCAGAATTCCATT GAATCTCGAGATTCAATGGAA TTCTGATGGCTTTTTG LAMP2A RV2: AATTCAAAAAGCCATCAGAATT CCATTGAATCTCGAGATTCAAT GGAATTCTGATGGC	This paper	N/A
shRNA targeting sequence: SCRBL FW: CCGGGTGGACTCTTGAAAGT ACTATCTCGAGATAGTACTTT CAAGAGTCCACTTTTTG SCRBL RV: AATTCAAAAAGTGGACTCTTG AAAGTACTATCTCGAGATAGT ACTTTCAAGAGTCCAC	This paper	N/A
Software and algorithms		
ImageJ	Schneider et al.[50]	https://imagej.nih.gov/ij/
Graphpad Prism 9.5.1	Dotmatics	https://www.graphpad.com

RESOURCE AVAILABILITY

Lead contact

To request resources, reagents and inquire for information, please email the lead contact, Saverio Minucci, at saverio.minucci@ieo.it.

Materials availability

This study did not generate new unique reagents.

Data and code availability

- Any additional information required to re-analyze the data reported in this paper is available from the lead contact upon request.
- All data reported in this paper will be shared by the lead contact upon request.
- This paper does not report original code.
- Any additional information required to reanalyze the data reported in this paper is available from the lead contact upon request.

EXPERIMENTAL MODEL AND STUDY PARTICIPANT DETAILS

Cell lines

HeLa (female origin) and HCT116 (male origin) cells were cultured in DMEM high glucose (ECM0103L, Euroclone) supplemented with 10% FBS (Microtech S.R.L.), at 37°C with 95% relative humidity and 5% CO_2. Cells are routinely checked and re-authenticated by the European Institute of Oncology (Italy) by genotyping random batches.

Xenograft tumor models

CD1 nude mice (8- to 10-weeks old females from Charles River) were subcutaneously injected with HCT116 cells (5×10^6 cells in 150 μL of PBS). After 10 days post injection, mice were randomly divided in experimental groups (5 mice per cage), monitored every alternate day and measured for tumor dimensions using calipers. Tumor volume was calculated by the following formula: $(A \times B^2)/2$, where A is the larger and B is the smaller of the two dimensions. IACS-010759 was administered every day at 9 am by oral gavage, and at 6pm food was replenished according to treatment (intermittent 24hrs fasting cycles, or *ad libitum* feeding). NAC has been dissolved in drinking water (1 g/L). At the end point (35 days post-implantation), mice were euthanized by CO_2 asphyxiation and autopsied. Tumors have been resected and weighed, and then collected in liquid nitrogen for further analysis. All the experiments have been performed under the EU regulatory standards with the project number 71/2019-PR authorized by the Ministry of Health, Italy.

METHOD DETAILS

In vitro treatment of cells in high and low glucose conditions

HeLa and HCT116 cells were plated at 200.000 cells/well in six well plates, and then treated with drugs, or left untreated as control, in DMEM containing 10 mM glucose and 10% FBS. After 24hrs, media were replenished with either DMEM containing 10 mM glucose and 10% FBS (HG), or DMEM containing 2.5mM glucose and 10% FBS (LG), with or without drugs, for additional 24hrs.

Knockdown and overexpression experiments

Viral constructs listed in the table below were used to transfect 293T (lentiviral constructs) or phoenix-AMPHO (retroviral constructs) packaging cells, following the manufacturer's protocol (Addgene). Viral particles were used to transduce target cells, which were then selected by appropriate antibiotic-containing media, or FACS-sorted when indicated (for GFP-expressing vectors). NDI1 overexpression and empty control vector (pLenti6.3_GFP) have been bought from Invitrogen. (Lb)NOX has been acquired from Addgene (pUC57-LbNOX) and subcloned in pLVX-puro (Clontech). Constructs for short hairpin RNAs were cloned in pLKO.1-puro (Addgene). CIP2A and MCL1 cDNAs were cloned into MSVC-puro (Addgene).

Immunoblotting

Primary antibodies were used at 1: 1000 dilution. Antibodies against α-tubulin, actin and vinculin were used as loading controls. All the secondary antibodies were used at 1: 10000 dilutions.

Immunofluorescence

HeLa cells were fixed with 4% paraformaldehyde for 20 min at RT, protected from the light. After three washes in PBS, cells were permeabilized with 0.3% Triton X-100 for 5 min, washed tree times with PBS and then blocked in 10% normal horse serum in PBS for 1 h at RT. Cells were stained at RT for 2 h with primary antibody against TOMM20 (1:200; Santa Cruz Biotech). After three washes (10 min, PBS), secondary antibody and DAPI were diluted in blocking solution and incubated for 1 h at RT, protected from the light. The coverslips were then mounted with kit provided mounting solution onto glass slides and images were acquired by Spinning disk confocal microscopy (SDCM) (Nikon Eclipse Ti2, CSU-W1 Confocal Scanner Unit) using NisElements 3.2 and analyzed using Fiji software.

Proximity ligation assay (PLA)

HeLa cells were seeded on round coverslips. Twenty-four hours after seeding, cells were treated with vehicle (DMSO) or IACS-010759, respectively. After the indicated treatments, cells were fixed and permeabilized with 0.3% Triton for 10 min at room temperature, washed three times with PBS, and then blocked with blocking reagent provided in the Duo-link PLA kit (DUO92101, Sigma-Aldrich). After blocking, cells were incubated for 2 h at room temperature with the two relevant primary antibodies diluted in antibody dilution buffer provided in PLA kit. The primary antibodies used were: mouse monoclonal anti-PP2A subunit C clone 1D6 05–421, Merck 1:400), rabbit polyclonal anti-CIP2A (ABC307, Merck 1:400). The PLA reactions (Duolink, Sigma-Aldrich) to detect anti-CIP2A and anti-PP2A antibodies used were performed according to manufacturer instructions. Images were acquired using a Leica DM6B microscope fitted with a PL Apo 63X/1.40 NA objective and PLA puncta were counted using an in house made macro with FIJI software.

Metabolic evaluations

Cells were plated in Seahorse XF96 plates (Agilent) at the density of 5×10^4 for HeLa, and 10×10^4 for HCT116 cells. Medium was then replaced with Seahorse base medium supplemented with glucose (either 10 or 2.5mM), pyruvate (1mM) and glutamine (2mM) at pH 7,4. We then followed manufacturer's protocol for subsequent measurements. When indicated, cells were permeabilized adding 0,05% digitonin prior to starting the Seahorse measurement.

Extracellular lactate or glucose concentrations were determined using two colorimetric-based kits, following manufacturer's instructions (Thermofisher). Ca^{2+} content was measured using FURA2 (Invitrogen) and a Tecan plate reader (Life Science). Cellular ROS content was measured by cellROX (Thermofisher) on a MACSQuant X flow cytometer (Miltenyi Biotech) or using AmplexRED (Thermofisher), fluorescence has been measured using GloMax plate reader (Promega).

QUANTIFICATION AND STATISTICAL ANALYSIS

Statistical analysis

All data are expressed as mean ± s.d, and subjected to a two-way ANOVA test with (*p < 0,1; **p < 0,05; ***p < 0,01; ****p < 0.005; ns non-significant). Statistical analysis has been performed using Graphpad prism software (Dotmatics) and it is reported in Figures and further described in Figures legends.